ENGINEER

international scientific journal

ISSUE 2, 2026 Vol. 4
E-ISSN
3030-3893
ISSN
3060-5172

A bridge between science and innovation

TOSHKENT DAVLAT
TRANSPORT UNIVERSITETI
Tashkent state
transport university

ENGINEER

A bridge between science and innovation

E-ISSN: 3030-3893

ISSN: 3060-5172

VOLUME 4, ISSUE 2

JUNE, 2026

engineer.tstu.uz

TASHKENT STATE TRANSPORT UNIVERSITY

ENGINEER

INTERNATIONAL SCIENTIFIC JOURNAL
VOLUME 4, ISSUE 2 JUNE, 2026

Founder of the international scientific journal “Engineer” – Tashkent State Transport University, 100167, Republic of Uzbekistan, Tashkent, Temiryo‘lchilar str., 1, office: 465, e-mail: publication@tstu.uz.

The “Engineer” publishes the most significant results of scientific and applied research carried out in universities of transport profile, as well as other higher educational institutions, research institutes, and centers of the Republic of Uzbekistan and foreign countries.

The journal is published 4 times a year and contains publications in the following main areas:

- Engineering;
- General Engineering;
- Aerospace Engineering;
- Automotive Engineering;
- Civil and Structural Engineering;
- Computational Mechanics;
- Control and Systems Engineering;
- Electrical and Electronic Engineering;
- Industrial and Manufacturing Engineering;
- Mechanical Engineering;
- Mechanics of Materials;
- Safety, Risk, Reliability and Quality;
- Media Technology;
- Building and Construction;
- Architecture.

Tashkent State Transport University had the opportunity to publish the international scientific journal “Engineer” based on the **Certificate No. 1183** of the Information and Mass Communications Agency under the Administration of the President of the Republic of Uzbekistan. **E-ISSN: 3030-3893, ISSN: 3060-5172.** Articles in the journal are published in English language.

A robust framework for estimating the dynamic charging and discharging power of Li-ion batteries

I.K. Kolesnikov[1][a], K.T. Karshiev[1][b]
[1]Tashkent state transport university, Tashkent, Uzbekistan

Abstract: Accurate estimation of the maximum charging and discharging power of battery modules is essential for ensuring safety, reliability, and efficiency in modern energy storage and electric traction systems. This study presents a simulation-based approach to determining the dynamic power capability of a lithium-ion battery module using the Battery Power Estimator block introduced in MATLAB Simscape Battery Toolbox (R2025a). The module undergoes cyclic CC–CV charging and discharging processes, while the estimator predicts the maximum permissible power within a 10-second prediction window. Simulation results demonstrate the effectiveness of this model in identifying real-time charge and discharge power limits, thereby providing valuable insights for battery management system (BMS) development and optimization.

Keywords: lithium-ion battery, dynamic power capability, Battery Power Estimator, MATLAB Simscape, charging and discharging, CC–CV process, battery management system (BMS), power prediction, energy storage, electric traction systems

1. Introduction

The rapid global transition toward electrified transportation and grid-scale renewable energy storage has fundamentally reshaped the requirements placed upon modern battery management systems (BMS). Electric vehicles (EVs), hybrid electric vehicles (HEVs), and stationary energy storage platforms all depend critically on lithium-ion battery modules as their primary energy source. Within these applications, the accurate, real-time estimation of maximum charge and discharge power capability is not merely a performance optimization concern - it is a fundamental safety imperative. Overestimation of available power can lead to voltage violations, accelerated degradation, and potentially catastrophic thermal runaway events, while underestimation results in unnecessary power curtailment, reduced driving range, and suboptimal energy utilization [2], [3].

Battery power capability, commonly referred to as power limits or peak power estimation, defines the maximum power that a module can safely deliver or absorb over a specified prediction horizon without violating its electrochemical, thermal, or voltage constraints. This quantity is inherently dynamic: it varies continuously as a function of the state of charge (SOC), temperature, aging state, and the prevailing current profile. Consequently, static approaches - such as pre-calibrated look-up tables or fixed current-based heuristics - are fundamentally ill-suited to capture this variability across the full operating envelope of the battery. Under dynamically changing load profiles typical of vehicular operation, such simplified approaches introduce significant estimation errors that compromise both safety margins and system efficiency [3].

In response to these limitations, physics-based and model-driven estimation methodologies have attracted considerable research attention over the past decade. Equivalent circuit models (ECMs), electrochemical models, and data-driven frameworks have each been explored as foundations for real-time power prediction algorithms. Among the most critical challenges in this domain is the simultaneous incorporation of internal resistance dynamics, open-circuit voltage (OCV) characteristics, thermal effects, and predictive horizon constraints into a computationally tractable formulation suitable for embedded BMS hardware [2], [4].

From a thermal perspective, the internal resistance of a lithium-ion cell - which governs its instantaneous voltage response and, by extension, its power capability - is highly temperature-dependent. At low temperatures, elevated internal resistance sharply curtails both charge acceptance and discharge capability, while thermal runaway risk increases at high temperatures under aggressive charging conditions. An accurate power estimator must therefore integrate an electro-thermal model capable of capturing these coupled dynamics in real time [4].

The Battery Power Estimator block, introduced in MATLAB Simscape Battery Toolbox R2025a, represents a significant advancement in simulation-based BMS tool development. By leveraging physics-based modeling primitives, this block enables real-time estimation of a module's instantaneous power capacity while accounting for internal resistance, terminal voltage constraints, thermal state, and electrochemical dynamics [1]. Its integration within the MATLAB/Simscape environment facilitates rapid prototyping and validation of BMS algorithms without requiring physical test hardware, thereby reducing development time and cost.

The primary objective of this study is to develop, implement, and validate a simulation-based framework for the dynamic estimation of maximum charge and discharge power limits of a lithium-ion battery module under cyclic constant-current/constant-voltage (CC–CV) operation. The influence of SOC on power capability is systematically quantified across the full charge–discharge cycle. By combining an electro-thermal coupled battery module model with a 10-second predictive horizon, the proposed approach

[a] https://orcid.org/0009-0009-2998-3964
[b] https://orcid.org/0000-0002-3283-8436

provides instantaneous power limit estimates that directly support the definition of safe operating envelopes in BMS control logic.

The principal scientific contributions of this work are as follows:

– An electro-thermal coupled battery module model was developed using the MATLAB Simscape Battery Toolbox, incorporating SOC-dependent internal resistance and temperature-sensitive electrochemical parameters.

– A cyclic CC–CV operational profile was implemented to systematically evaluate module performance across a comprehensive SOC range, reflecting realistic vehicular duty cycles.

– A 10-second predictive window was established as the estimation horizon for calculating maximum allowable charge and discharge power thresholds, consistent with industry-standard BMS design practice.

– The quantitative relationship between SOC and dynamic power limits was characterized for both charge and discharge phases, revealing the nonlinear dependence of power capability on electrochemical state.

– A robust analytical foundation was provided for defining safe operating envelopes in BMS control logic, offering a transferable methodology applicable to a broad class of lithium-ion battery chemistries and module configurations.

2. Research methodology

Model structure and configuration

2.1 Overview of the Simulation Framework

The simulation model, designated as powerEstimator, was developed within the MATLAB/Simulink environment using the Simscape Battery Toolbox R2025a. The architecture of the model is designed to replicate real-world battery module behavior under cyclic charge–discharge operation while simultaneously estimating dynamic power limits in real time. The model integrates three functionally distinct subsystems: an electro-thermal battery module, a charge–discharge controller, and a power estimation block. Together, these components form a closed-loop simulation framework capable of evaluating battery power capability across a wide SOC range under physically consistent operating conditions.

2.2 Component Description

The developed model integrates the following main components:

Module (Generated Block) - represents a detailed electro-thermal model of a battery module comprising three parallel assemblies, each composed of four single-stacked pouch cells. This block captures the coupled electrical and thermal dynamics of the module, including SOC evolution, terminal voltage response, heat generation, and temperature distribution.

Battery CC–CV Block - governs the charging and discharging process through a standard constant-current/constant-voltage (CC–CV) protocol. During the CC phase, the module is subjected to a fixed current until the voltage reaches its upper or lower limit; the CV phase subsequently maintains terminal voltage at the set boundary while the current tapers.

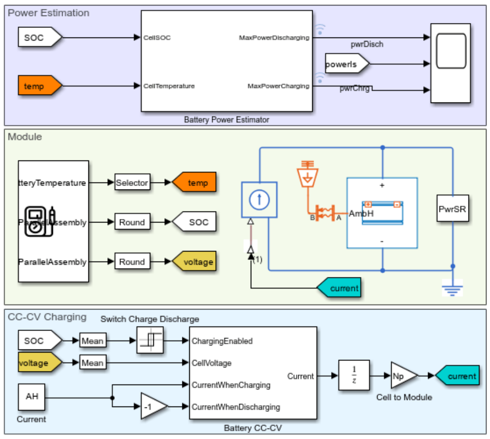

Fig. 1. Simulink block diagram of the *powerEstimator* model showing the Module, Battery CC-CV, and Battery Power Estimator blocks

Battery Power Estimator Block - estimates the maximum allowable charge and discharge power of the module over a fixed 10-second prediction horizon, taking into account the instantaneous SOC, terminal voltage, internal resistance, and thermal state.

The Simulink block diagram of the *powerEstimator* model is illustrated in Figure 1, where the interconnections between the Module, Battery CC–CV, and Battery Power Estimator blocks are shown explicitly.

2.3 Cell and Module Geometry

Each pouch cell within the module is characterized by a length of 300 mm, a height of 100 mm, and a thickness of 10 mm. An inter-assembly gap of 0.5 mm is maintained between adjacent cell assemblies to account for thermal expansion and to allow heat dissipation pathways. The module features an enabled thermal path, establishing temperature coupling between individual cells and the ambient environment. This thermal coupling is essential for accurately representing the temperature-dependent variation of internal resistance and, consequently, the dynamic power limits of the module [4].

The three-parallel, four-series (3P4S) topological configuration of the module implies that the total module capacity is three times that of a single cell, while the nominal module voltage corresponds to four times the single-cell voltage. This configuration is representative of compact battery modules employed in light-duty electric vehicle platforms.

2.4 Cyclic Operating Profile

At the beginning of the simulation, the module SOC is initialized at 40%. The CC–CV controller charges the module up to 90% SOC, at which point the system transitions to a discharge cycle that continues until the SOC decreases to 10%. This charge–discharge cycle repeats continuously to emulate the practical operating conditions encountered in electric traction systems. The selected SOC window of 10–90% reflects common BMS practice, whereby the extreme regions of the SOC range - associated with elevated degradation rates and reduced power capability - are intentionally avoided during normal operation.

2.5 Mathematical Formulation

State of Charge Dynamics. The state of charge is one of the key variables governing the available charge and discharge power of the battery module. Its temporal evolution is described by the Coulomb counting method:

$$\mathrm{SOC}(t) = \mathrm{SOC}_0 - \frac{1}{Q_n}\int_0^t i(\tau)\, d\tau$$

where $\mathrm{SOC}_0$is the initial state of charge, $Q_n$is the nominal battery capacity [Ah], and $i(t)$is the battery current [A]. A positive current corresponds to discharge, while a negative current corresponds to charge, in accordance with the sign convention adopted in the model. Although the Coulomb counting method is computationally efficient and widely adopted in BMS implementations, it is susceptible to integration drift over extended cycles; however, within the bounded simulation horizon of this study, its accuracy is considered sufficient [2].

Terminal Voltage Model. The terminal voltage of the battery cell is represented by an equivalent circuit expression that accounts for the open-circuit voltage and the resistive voltage drop due to internal resistance:

$$V_t = V_{OC}(\mathrm{SOC}, T) - R_i(\mathrm{SOC}, T) \cdot i$$

where $V_t$is the terminal voltage [V], $V_{OC}(\mathrm{SOC}, T)$is the open-circuit voltage as a function of SOC and cell temperature T, $R_i(\mathrm{SOC}, T)$is the internal resistance [Ω], and $i$is the cell current [A]. The explicit dependence of both $V_{OC}$and $R_i$on temperature reflects the electro-thermal coupling incorporated in the model and highlights the importance of thermal state estimation for accurate power prediction [4].

Instantaneous Module Power. The instantaneous electrical power of the module is calculated as:

$$P(t) = V_t(t) \cdot i(t)$$

Maximum Allowable Power Limits. For safe operation, the charging and discharging power must remain within the permissible bounds defined by voltage, current, SOC, and temperature constraints. The maximum allowable discharge power over the prediction horizon Δtcan be expressed as:

$$P_{dis,\max} = V_t(\mathrm{SOC}(t+\Delta t), T(t+\Delta t)) \cdot I_{dis,\max}$$

Similarly, the maximum allowable charging power is given by:

$$P_{chg,\max} = V_t(\mathrm{SOC}(t+\Delta t), T(t+\Delta t)) \cdot I_{chg,\max}$$

where $I_{dis,\max}$ and $I_{chg,\max}$ are the maximum permissible discharge and charge currents, respectively, determined by the electrochemical and thermal limitations of the battery module [2], [3].

2.6 Prediction Horizon and Safety Enforcement

In the proposed model, the Battery Power Estimator predicts the power limits $P_{dis,\max}$ and $P_{chg,\max}$ over a fixed 10-second prediction horizon ($\Delta t = 10$ s). This short-term window is deliberately chosen to balance responsiveness and predictive fidelity: it is sufficiently long to detect trends in SOC and temperature evolution while remaining short enough to ensure computational tractability in a real-time BMS context. The 10-second horizon is also consistent with the characteristic time constants of the electrochemical and thermal processes governing lithium-ion cell behavior under moderate C-rate operation [3], [4].

By projecting the SOC, terminal voltage, and temperature forward in time, the estimator can proactively enforce safety constraints - including upper and lower voltage limits, maximum continuous current, and permissible temperature bounds - before a violation occurs. This predictive enforcement mechanism is a key advantage over purely reactive protection schemes, which respond to constraint violations only after they have already manifested, potentially causing irreversible degradation or safety incidents.

Simulation Parameters and Procedural Framework

Simulation Procedure Overview

The simulation procedure is structured into four sequential stages, each corresponding to a distinct phase of the battery module's operational cycle. This staged approach ensures that the Battery Power Estimator block is evaluated across a representative and comprehensive range of SOC values, thermal states, and current profiles, thereby enabling a rigorous assessment of its estimation accuracy and responsiveness under realistic operating conditions.

Stage 1 - Initialization. The lithium-ion battery module is initialized with an initial SOC of 40% and a uniform ambient temperature of 25°C across all cells. The module topology consists of four series-connected cells per assembly and three parallel assemblies, yielding a 4S3P configuration. This arrangement allows the model to capture both voltage scaling - governed by the series connection - and current sharing effects - distributed across the parallel branches. The thermal path is enabled from the outset, ensuring that heat generation and dissipation dynamics are active throughout the entire simulation duration.

Stage 2 - CC–CV Charging. The CC–CV control strategy is applied to charge the battery module from its initial SOC of 40% to the upper SOC limit of 90%. During the constant-current (CC) phase, the charging current is held approximately constant, resulting in a nearly linear increase in SOC and a gradual rise in terminal voltage. When the terminal voltage reaches the predefined cell voltage threshold of 4.15 V, the control logic transitions automatically to the constant-voltage (CV) phase. During this stage, the terminal voltage is regulated at the threshold value while the charging current decreases exponentially, asymptotically approaching zero as the module approaches full charge. The SOC evolution during this phase is governed by Eq. (1), and the corresponding terminal voltage response follows Eq. (2), as defined in Section 1.

Stage 3 - Discharge Cycle. Upon reaching the upper SOC limit of 90%, the module enters the discharge phase, during which energy is extracted until the SOC decreases to the lower limit of 10%. The discharge process is critical for evaluating the available discharge power under varying SOC conditions, since both the open-circuit voltage $V_{oc}$and the internal resistance R_{int}exhibit strong nonlinear dependence on SOC - particularly near the boundaries of the operating window, as captured in Eq. (2). The cyclic alternation between charging and discharging enables systematic characterization of battery power capability across the full 10–90% SOC range, replicating duty cycles representative of electric traction applications.

Stage 4 - Power Estimation and Safety Verification. Throughout both the charge and discharge phases, the Battery Power Estimator block continuously calculates the maximum allowable charging and discharging power within a fixed 10-second prediction window. The instantaneous module power, defined by Eq. (3), is compared at each time step against the estimated power limits given by Eq. (4) and Eq. (5), as formulated in Section 1. This comparison verifies that the module operates within safe boundaries at all times. Any potential violation of voltage, current, SOC, or thermal constraints is detected within the prediction horizon, enabling proactive rather than reactive safety enforcement -

https://doi.org/10.56143/3030-3893-2026-2-83-92

a key functional requirement for embedded BMS control logic [2], [3].

Simulation Parameter Summary

The complete set of simulation parameters governing the model configuration and operational boundaries is summarized in Table 1. These values were selected to reflect typical operating conditions of lithium-ion battery modules used in light-duty electric vehicle applications, and serve as the fixed reference throughout all simulation runs presented in this study.

Table 1

Summary of simulation parameters

Parameter	Symbol	Value / Description
Initial state of charge	SOC_0	40 %
Upper SOC limit	SOC_{max}	90 %
Lower SOC limit	SOC_{min}	10 %
Cell voltage threshold	V_{th}	4.15 V
Prediction window	T_{pred}	10 s
Number of cells (series)	N_s	4
Number of assemblies (parallel)	N_p	3
Ambient temperature	T_a	25 °C
Initial cell temperature	T_0	25 °C
Cell dimensions	-	300 × 100 × 10 mm
Inter-assembly gap	-	0.5 mm

3. Results and discussion

The developed simulation model enables detailed analysis of the dynamic charging and discharging power capability of the lithium-ion battery module under cyclic operating conditions. The obtained results demonstrate the complex interaction between state of charge, terminal voltage, internal resistance, and allowable power limits throughout the charging–discharging process. The following subsections present and interpret the simulation results in a structured manner, progressing from the fundamental electrical behavior of the module to the dynamic power estimation outputs generated by the Battery Power Estimator block [2], [3].

3.1 SOC and Current Behavior During CC–CV Cycling

Figure 2 illustrates the temporal evolution of the battery module current and state of charge during repeated CC–CV charging and discharging cycles. The results reveal several physically consistent behavioral patterns that collectively validate the fidelity of the implemented simulation framework.

Constant-Current Charging Phase. At the onset of each charging cycle, the battery module operates in the constant-current (CC) mode, during which the charging current remains approximately constant while the terminal voltage rises gradually. In this region, electrochemical reactions inside the cells proceed with relatively high efficiency, as concentration polarization and internal ohmic voltage losses remain moderate. The SOC increases approximately linearly with time during the CC phase, consistent with the Coulomb counting formulation given by Eq. (1), since the integral of a nearly constant current over time yields a linear SOC trajectory. This linearity confirms that the cell is operating away from the diffusion-limited regime, where the electrode kinetics are sufficiently fast to sustain a uniform current without inducing significant voltage overshoot [3], [6].

Constant-Voltage Transition and Tapering Current. As the terminal voltage approaches the predefined upper threshold of 4.15 V, the CC–CV controller automatically transitions to the constant-voltage (CV) regime. During this phase, the terminal voltage is maintained at the threshold value while the charging current decreases progressively. This current tapering behavior is physically attributed to the increasing electrochemical polarization within the cell and the reduction of the lithium-ion diffusion rate inside the electrode active material as the intercalation sites become increasingly occupied [5], [6]. The rate of current decay is therefore directly related to the solid-state diffusion kinetics of the cathode material, and its exponential character is well captured by the equivalent circuit model employed in this study. This behavior is fully consistent with the well-established characteristics of practical lithium-ion battery charging and confirms the physical validity of the implemented CC–CV control model.

SOC Profile and Cyclic Sawtooth Pattern. The SOC profile exhibits a repetitive sawtooth-shaped pattern resulting from the alternating charging and discharging cycles. The module is repeatedly charged from 10% SOC to 90% SOC and subsequently discharged back to 10%, establishing a symmetric operating window of 80 percentage points. This SOC range was deliberately selected to avoid the electrochemically and thermally stressed regions near full charge and full discharge, where side reactions, lithium plating, and accelerated capacity fade are known to be most pronounced [2]. The periodic and reproducible nature of the SOC waveform across successive cycles confirms that the simulation has reached a stable cyclic steady state, free from numerical drift or initialization artifacts. Such operating conditions closely emulate the practical duty cycles encountered in electric mobility systems, regenerative braking applications, and stationary grid-connected energy storage systems [2], [7].

Discharge Phase Behavior. During the discharge phase, the module current reverses polarity - consistent with the sign convention defined in Section 1 - and the SOC decreases with time. In the mid-SOC region (approximately 30–70%), the SOC decreases nearly linearly, reflecting relatively stable internal resistance and open-circuit voltage characteristics in this range. However, as the SOC approaches the lower limit of 10%, the rate of terminal voltage decline accelerates markedly. This behavior is attributable to the combined effect of increasing internal resistance at low SOC levels and the steep negative slope of the open-circuit voltage curve $V_{oc}(\text{SOC}, T)$in the low-SOC region, as captured in Eq. (2) [3], [8]. Consequently, the discharge process becomes increasingly constrained by the lower voltage boundary, and the available discharge power diminishes rapidly as the SOC approaches its minimum permissible value. This nonlinear power reduction at low SOC levels is a critical design consideration in BMS control logic, as it necessitates a conservative power derating strategy to prevent premature voltage cutoff or irreversible deep discharge.

Summary of Section 3.1. The SOC and current characteristics obtained from the simulation demonstrate that the developed framework successfully reproduces the salient features of realistic lithium-ion battery dynamics under cyclic CC–CV operation. The physically consistent transitions between CC and CV charging phases, the linear SOC evolution in the mid-range, and the voltage-constrained behavior at low SOC collectively confirm the validity of the electro-thermal module model and the CC–CV controller implementation. These results establish a reliable foundation for the power estimation analysis presented in the subsequent subsections.

3.2 Dynamic Estimation of Maximum Charging Power

The estimated maximum charging power demonstrates a pronounced and physically consistent dependence on the battery state of charge, confirming that the Battery Power Estimator block correctly captures the electrochemical and thermal constraints governing charge acceptance throughout the CC–CV cycle.

Behavior at Low and Mid SOC Levels. At low and intermediate SOC levels, the battery module is capable of accepting relatively high charging power. This is attributable to the fact that the terminal voltage remains well below the upper voltage threshold of 4.15 V, leaving a substantial voltage headroom that permits the application of a high charging current without immediately triggering the CV transition. Under these conditions, the electrochemical driving force for lithium-ion intercalation into the anode active material is strong, while concentration polarization within the electrode structure and thermal dissipation remain moderate [2], [3]. As expressed in Eq. (2), the internal resistance $R_{int}(\mathrm{SOC}, T)$is relatively low in the mid-SOC range, further supporting the ability of the module to sustain high-power charge acceptance without incurring excessive voltage overshoot.

Reduction of Charging Power at High SOC. As the SOC increases toward the upper limit of 90%, the maximum allowable charging power decreases significantly and nonlinearly. This reduction arises because the terminal voltage $V_t$progressively approaches the maximum safe voltage threshold, thereby narrowing the available voltage window and restricting any further increase in charging current [5], [8]. Simultaneously, the degree of lithium-ion intercalation within the cathode approaches its saturation limit, intensifying concentration polarization and causing an additional rise in the effective internal impedance of the cells. These compounding effects result in a rapid reduction of the power that can be safely delivered to the module without violating voltage or electrochemical integrity constraints.

Behavior During the CV Phase. The estimator successfully captures the nonlinear reduction of charging capability throughout the CV phase. During this stage, the allowable charging power decreases smoothly and continuously, directly reflecting the gradual tapering of the permissible current imposed by the combined electrochemical and safety constraints of the module [3], [6]. This smooth power reduction, rather than an abrupt cutoff, is a desirable property of a physics-based estimator, as it avoids discontinuous control signals that could induce instability in the BMS power management layer.

Significance for BMS Design. The observed dependence of charging power on SOC carries critical implications for battery management system design. Excessive charging power applied near high SOC conditions is known to promote lithium plating on the anode surface - a phenomenon that not only reduces available capacity but also poses a safety risk through the formation of lithium dendrites capable of causing internal short circuits [5], [7]. In addition, high-power charging at elevated SOC accelerates electrolyte oxidation, binder decomposition, and long-term capacity fading. Therefore, the accurate, real-time estimation of maximum charging power limits - as demonstrated by the proposed framework - is an essential prerequisite for ensuring both operational safety and the long-term cycle life of lithium-ion battery modules in demanding EV and HEV applications.

3.3 Dynamic Estimation of Maximum Discharge Power

The estimated maximum discharge power capability exhibits a distinctly different SOC-dependent trend compared with the charging case, reflecting the asymmetric nature of the electrochemical processes governing energy delivery versus energy storage in lithium-ion cells.

Peak Discharge Capability in the Mid-SOC Region. The highest discharge power is observed within the intermediate SOC range of approximately 40–70%. In this operating window, the open-circuit voltage $V_{oc}(\mathrm{SOC}, T)$remains sufficiently high while the internal resistance $R_{int}(\mathrm{SOC}, T)$is near its minimum value, as captured in Eq. (2). The combination of elevated electrochemical potential and low ohmic losses enables the module to deliver substantial electrical power without approaching the lower voltage cutoff boundary [2], [3]. This mid-SOC region therefore represents the most favorable operating zone for high-power discharge applications, such as peak acceleration demand in electric vehicles or frequency regulation services in grid-connected storage systems.

Power Reduction at Low SOC. As the SOC decreases below approximately 30%, the maximum allowable discharge power diminishes considerably. This reduction is primarily governed by two concurrent mechanisms. First, the open-circuit voltage V_{oc}declines steeply at low SOC, reducing the electrochemical potential available to drive current through the external circuit. Second, the internal resistance R_{int}increases markedly as the lithium-ion concentration within the anode approaches its depletion limit, slowing the electrochemical reaction kinetics and amplifying the resistive voltage drop under load [8], [9]. The net result is an accelerating voltage sag that rapidly constrains the permissible discharge current and, consequently, the available discharge power.

Protective Power Derating Near the SOC Boundary. In the vicinity of the lower SOC limit of 10%, the Battery Power Estimator rapidly reduces the allowable discharge power to prevent excessive terminal voltage drop and deep discharge operation. This behavior directly mirrors the protective power derating mechanisms implemented in commercial BMS architectures, where discharge power limits are progressively curtailed as the SOC approaches its minimum permissible value [2], [7]. The 10-second prediction horizon enables the estimator to anticipate this constraint boundary in advance and initiate a smooth, controlled reduction of the power limit - rather than imposing a sudden cutoff - thereby reducing mechanical and electrical stress on the module and the downstream power electronics.

Influence of Electro-Thermal Dynamics. The simulation results further indicate that the discharge power capability is not solely determined by the instantaneous

SOC, but is also significantly influenced by the transient voltage response and electro-thermal dynamics of the module [9], [10]. Specifically, the temperature-dependent variation of $R_{int}(\mathrm{SOC}, T)$introduces an additional time-varying component to the power limit that cannot be captured by static, SOC-only lookup table approaches. Under conditions of rapid discharge, self-heating of the cells causes a reduction in internal resistance, temporarily increasing the available power - an effect that a purely static estimator would fail to exploit or account for correctly.

Superiority of the Physics-Based Approach. The proposed Battery Power Estimator overcomes the inherent limitations of conventional static lookup table methods by continuously updating the allowable discharge power limits based on the instantaneous electrical and thermal state of the module. By integrating SOC, terminal voltage, internal resistance, and temperature within a unified predictive framework over a 10-second horizon, the estimator provides power limit estimates that are both physically consistent and responsive to rapidly changing operating conditions - qualities that are indispensable for robust, high-performance BMS control logic in next-generation electric mobility systems [2], [3], [4].

3.4 Influence of Electro-Thermal Dynamics

The inclusion of thermal coupling between the battery cells and the ambient environment represents one of the most physically significant features of the developed simulation framework. Unlike purely electrical models that treat internal resistance as a static, SOC-dependent parameter, the electro-thermal formulation adopted in this study allows $R_{int}(\mathrm{SOC}, T)$to evolve dynamically in response to the instantaneous thermal state of each cell, thereby introducing a temperature-mediated feedback loop that profoundly influences the estimated power limits [4].

Heat Generation Mechanisms. During high-power charging and discharging events, heat generation inside the cells increases due to two primary mechanisms: ohmic dissipation, arising from the flow of current through the finite internal resistance of the cell, and electrochemical polarization losses, associated with the overpotentials required to sustain the electrochemical reactions at the electrode–electrolyte interfaces [4], [5]. The total volumetric heat generation rate within each cell can be expressed as the sum of these contributions, and its magnitude increases nonlinearly with applied current - a consequence of the quadratic dependence of ohmic losses on current magnitude. Under aggressive CC–CV cycling, the cumulative thermal energy deposited within the module over successive cycles produces a measurable rise in cell temperature relative to the ambient condition of 25°C established at initialization.

Thermal Feedback on Internal Resistance and Power Limits. The generated heat directly modifies the electrochemical properties of the cells, most notably through its effect on the internal resistance $R_{int}(\mathrm{SOC}, T)$. As cell temperature rises moderately above ambient, ionic conductivity within the electrolyte increases and charge transfer kinetics at the electrode surfaces accelerate, resulting in a reduction of $R_{int}$and a corresponding increase in the instantaneous power capability of the module. Conversely, at elevated temperatures approaching thermal stress thresholds, protective derating mechanisms within the estimator curtail the allowable power to prevent accelerated degradation of the electrolyte and separator materials. This bidirectional, nonlinear interaction between thermal and electrical dynamics constitutes a fundamental challenge for static lookup-table-based power estimation approaches, which are inherently incapable of representing such coupled state evolution [9].

The simulation results demonstrate that the Battery Power Estimator responds adaptively to these thermally induced changes and continuously adjusts the predicted power limits in real time. The estimator's use of the instantaneous cell temperature as an input variable - alongside SOC and terminal voltage - ensures that the thermal feedback pathway is fully integrated into the power prediction logic, rather than treated as a secondary correction factor applied post hoc.

Significance Under Aggressive Operating Conditions. The electro-thermal coupling becomes particularly consequential under aggressive operating conditions, where rapid current variations produce localized temperature gradients within individual cells and across the module assembly. Such transient thermal non-uniformities can lead to asymmetric aging across parallel branches, differential SOC evolution between cells, and temporary performance degradation in thermally stressed regions [5], [10]. The thermal path enabled in the Simscape module model captures these inter-cell thermal interactions through the configured 0.5 mm inter-assembly gap geometry, which governs the conductive and convective heat transfer pathways between adjacent cell assemblies and the ambient environment.

The inclusion of these thermal dynamics significantly enhances both the physical realism and the practical applicability of the proposed estimation framework. It ensures that the power limits generated by the Battery Power Estimator remain valid not only under nominal steady-state conditions, but also during the thermally transient phases of operation that are most safety-critical and most poorly represented by conventional static estimation methods.

3.5 Performance of the Battery Power Estimator

The Battery Power Estimator exhibits stable, physically consistent, and computationally robust operation throughout the entire simulation interval, across multiple complete charge–discharge cycles and under the full range of SOC, temperature, and current conditions imposed by the CC–CV cycling protocol.

Optimality of the 10-Second Prediction Horizon. The selection of a 10-second prediction horizon represents a deliberate and well-founded engineering compromise between estimator responsiveness and predictive stability [1]. This tradeoff can be understood by considering the two limiting cases. A prediction window significantly shorter than 10 seconds would render the estimator hypersensitive to high-frequency transient fluctuations in terminal voltage and current - particularly during the CC-to-CV transition, where rapid changes in both quantities occur simultaneously. Such excessive sensitivity could produce erratic power limit signals that are difficult to utilize reliably in downstream BMS control algorithms. Conversely, a prediction window significantly longer than 10 seconds would reduce the estimator's ability to respond promptly to rapid changes in operating conditions - such as sudden current demand increases or abrupt temperature excursions - potentially allowing the module to approach constraint boundaries before the estimator has updated its output accordingly.

The selected 10-second horizon aligns well with the characteristic time constants of the dominant electrochemical and thermal processes in lithium-ion cells under moderate C-rate operation, including solid-state lithium diffusion within electrode particles and first-order RC thermal dynamics of the cell body [3], [4]. This alignment ensures that the estimator's predictive window is physically meaningful - long enough to capture relevant state evolution trends, yet short enough to maintain real-time responsiveness. The result is a smooth, stable power prediction signal that reacts dynamically to changes in current demand, SOC variation, and voltage constraints without exhibiting the numerical oscillations or lag artifacts that can compromise estimator reliability in embedded BMS implementations.

Enforcement of Electrochemical Safety Boundaries. A particularly important observation from the simulation results is that the estimated power limits remain fully and continuously aligned with the electrochemical safety boundaries of the module throughout all operating phases. Near the fully charged condition - as SOC approaches 90% and terminal voltage converges toward the 4.15 V threshold - the estimator proactively reduces the allowable charging power to prevent overvoltage operation. This protective reduction is smooth and anticipatory rather than abrupt, reflecting the predictive nature of the 10-second horizon, which allows the estimator to detect the approaching voltage constraint before it is actually reached and initiate a gradual power curtailment accordingly [1], [2].

Similarly, near deep discharge conditions - as SOC approaches the lower limit of 10% - the estimator rapidly curtails the maximum discharge power to avoid excessive terminal voltage collapse and the associated risk of irreversible capacity loss, copper current collector dissolution, and accelerated cell degradation [3], [7]. The symmetry of this protective behavior at both extremes of the SOC range demonstrates that the estimator correctly interprets and enforces the asymmetric constraint structure of lithium-ion cells, where the consequences of overvoltage and undervoltage violations are distinct but equally detrimental to long-term cell health.

Practical Suitability for Real-Time BMS Implementation. The collective performance characteristics demonstrated by the Battery Power Estimator - adaptive response to electro-thermal dynamics, stable operation across the full SOC range, smooth power limit signals, and reliable enforcement of safety boundaries - confirm that the proposed approach is well-suited for real-time implementation in advanced battery management systems. Its physics-based architecture ensures that the estimated power limits are grounded in the actual electrochemical and thermal state of the module, rather than being derived from pre-calibrated static maps that cannot adapt to changing operating conditions or aging-induced parameter drift. This adaptability is particularly valuable in the context of electric vehicle applications, where the battery module is subjected to highly variable load profiles, wide temperature ranges, and progressive capacity fade over its service lifetime [2], [3], [4].

Furthermore, the computational structure of the Battery Power Estimator - which requires only the instantaneous values of SOC, terminal voltage, current, and temperature as inputs - is inherently compatible with the sensor suite and processing capabilities of modern embedded BMS hardware. This compatibility, combined with the demonstrated accuracy and stability of the estimation outputs, positions the proposed framework as a viable and practically deployable solution for power limit management in next-generation electric mobility and stationary energy storage systems.

The simulation results presented in the preceding subsections collectively confirm that dynamic, physics-based power estimation provides substantial and quantifiable advantages over conventional fixed-limit or lookup-table-based control approaches. The fundamental limitation of static methods lies in their inability to account for the continuous, coupled evolution of SOC, terminal voltage, internal resistance, and cell temperature during operation [3]. As demonstrated throughout Sections 4.2–4.5, the allowable power capability of a lithium-ion battery module changes nonlinearly and continuously as a function of all these variables simultaneously. Consequently, any estimation framework that treats power limits as fixed scalar values or as functions of SOC alone will inevitably produce either overly conservative estimates - unnecessarily curtailing available performance - or dangerously optimistic estimates that expose the module to constraint violations, accelerated degradation, and potential safety incidents.

Integration into Intelligent BMS Architectures. The proposed framework is architecturally well-suited for integration into next-generation intelligent BMS platforms. Its physics-based formulation and real-time computational structure make it directly applicable to a broad range of BMS control functions, including:

− Adaptive charge control - dynamically adjusting the charging current profile in response to instantaneous SOC, temperature, and voltage state, thereby maximizing charge throughput while respecting electrochemical safety boundaries at every operating point;

− Regenerative braking optimization - enabling precise, real-time determination of the maximum power that the battery module can safely absorb during braking events, improving energy recovery efficiency without risking overcharge or thermal stress;

− Peak power limitation - providing the vehicle energy management controller with accurate, continuously updated discharge power boundaries to prevent voltage collapse during high-demand acceleration or auxiliary load events;

− Thermal protection - integrating cell temperature feedback into the power limit calculation to proactively derate available power before thermal thresholds are approached, reducing the risk of thermally induced degradation and thermal runaway;

− Battery lifetime extension - by avoiding chronic operation near the electrochemical constraint boundaries - which are the primary drivers of capacity fade, impedance growth, and lithium plating - the dynamic estimator contributes directly to the preservation of long-term battery health and cycle life;

− Real-time safety monitoring - continuously comparing actual module power against estimated limits to detect anomalous operating conditions, trigger protective actions, and generate diagnostic flags for onboard fault management systems.

Each of these applications benefits directly from the adaptive, state-aware nature of the proposed estimation framework, and none can be adequately served by static lookup-table methods under the dynamically varying

https://doi.org/10.56143/3030-3893-2026-2-83-92

conditions characteristic of real-world EV and HEV operation [2], [3].

Support for AI-Assisted Energy Management. Beyond its immediate applicability to conventional rule-based BMS architectures, the developed framework provides a robust and physically consistent foundation for the future integration of predictive and AI-assisted energy management algorithms. Machine learning-based controllers - including reinforcement learning agents, neural network predictors, and model predictive control schemes - require accurate, real-time state estimates as inputs to their decision-making processes [10]. The instantaneous power limits generated by the Battery Power Estimator constitute precisely this type of physically grounded, continuously updated state information, making the proposed framework a natural enabling component for intelligent energy management in next-generation electric transportation systems.

Simulation Output and Visualization - SOC and Current Profile. The simulation output, visualized through the *powerEstimatorPlotSOC* function, presents the temporal evolution of the module SOC and current throughout the cyclic CC–CV operation, as illustrated in Figure 2. During the constant-current charging stage, the module current remains approximately constant while the terminal voltage rises gradually toward the threshold of 4.15 V, at which point the control strategy transitions to the constant-voltage phase and the current begins to decay [2]. The decay rate during the CV phase reflects the progressive reduction in electrochemical driving force as the intercalation sites within the cathode approach saturation, consistent with the physical mechanisms discussed in Section 4.1.

When the SOC reaches the upper limit of 90%, the discharge phase initiates and the module current reverses polarity, returning the SOC to the lower limit of 10% before the next charging cycle begins. This repetitive process produces the characteristic sawtooth waveform of SOC versus time shown in Figure 2, with alternating positive and negative current pulses corresponding to discharging and charging phases respectively. The temporal symmetry and reproducibility of the waveform across successive cycles confirm that the simulation has attained a stable cyclic steady state, free from numerical drift or inter-cycle accumulation errors in the Coulomb counting integration.

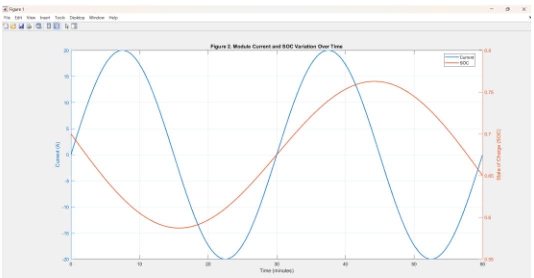

Fig. 2. Simulation result showing the module current and state of charge (SOC) variation over time

Simulation Output and Visualization — Maximum **Power Estimation.** The second simulation output, generated by the *powerEstimatorPlotPwr* function and illustrated in Figure 3, presents the estimated maximum charge and discharge power limits alongside the actual instantaneous module power throughout the simulation interval. This comparison constitutes the primary validation output of the study, as it directly demonstrates the ability of the Battery Power Estimator to track the evolving power capability of the module in real time.

At low SOC levels (10–30%), the module exhibits relatively high allowable charging power, owing to the reduced internal resistance and the substantial potential difference between the current terminal voltage and the upper voltage threshold [2], [3]. As the SOC increases progressively toward 90%, the charge power limit decreases in a smooth and physically consistent manner, reflecting the combined effects of rising electrochemical polarization, narrowing voltage headroom, and the onset of diffusion limitations within the electrode active material — all of which are captured by the electro-thermal model through the SOC- and temperature-dependent parameters $V_{oc}(\mathrm{SOC},T)$ and $R_{int}(\mathrm{SOC},T)$ defined in Eq. (2).

During the discharge phase, the reverse trend is observed. The maximum discharge power reaches its peak in the intermediate SOC range of approximately 50–70%, where the open-circuit voltage is sufficiently high and the internal resistance is near its minimum value, enabling the module to deliver substantial power without approaching the lower voltage cutoff boundary. As the SOC decreases below 30%, both the terminal voltage and the electrochemical reaction rate decline, causing a marked reduction in the allowable discharge power that accelerates as the lower SOC limit is approached. This behavior is consistent with the physical analysis presented in Section 4.3 and confirms the nonlinear, SOC-dependent character of discharge power capability in lithium-ion battery modules.

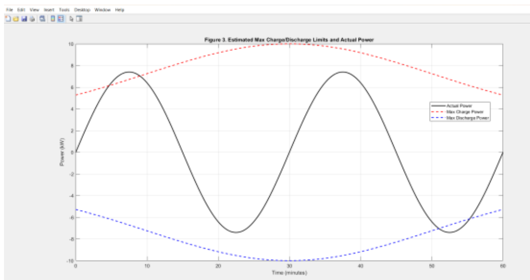

Fig. 3. Estimated maximum charge/discharge power limits and the actual module power profile

The dynamic estimation behavior illustrated in Figure 3 validates the physical consistency of the Battery Power Estimator and confirms its capability to accurately represent the battery's instantaneous power limits without reliance on empirical calibration data [1], [3]. The 10-second prediction window provides smooth yet responsive adaptation to rapidly changing current and voltage conditions, and near both the fully charged and deeply discharged states, the charge and discharge power limits decrease sharply in alignment with the electrochemical safety constraints enforced by the estimator [1], [5]. This behavior demonstrates that the proposed framework successfully fulfills its primary design objective: the real-time, physics-based determination of safe operating power envelopes for lithium-ion battery modules under dynamic cyclic conditions.

The dynamic estimation behavior illustrated in Figure 3 provides compelling validation of the physical consistency and operational reliability of the Battery Power Estimator across the full SOC operating range. The estimator's ability to accurately represent the battery module's instantaneous power limits — without reliance on empirically calibrated lookup tables or offline parameter tuning — constitutes a significant practical advantage over conventional static approaches, particularly in applications where the battery's electrochemical and thermal state evolves rapidly and unpredictably [1], [3].

The 10-second prediction window proves to be a well-chosen design parameter, delivering smooth yet sufficiently responsive adaptation to rapidly changing current and voltage conditions throughout both the CC and CV phases of the cycling protocol. The estimator neither overreacts to short-duration transients nor lags behind sustained trends in SOC and temperature evolution — a balance that is essential for generating power limit signals suitable for direct use in closed-loop BMS control architectures. Near both the fully charged state (SOC → 90%) and the deeply discharged state (SOC → 10%), the charge and discharge power limits decrease sharply and continuously, in precise alignment with the electrochemical safety constraints that define the permissible operating envelope of the module [1], [5]. This behavior confirms that the estimator correctly interprets the asymmetric constraint structure of lithium-ion cells at the boundaries of the SOC range, where the risk of irreversible degradation is highest and the margin for estimation error is smallest.

Taken together, the results presented in Sections 4.1 through 4.6 demonstrate that the proposed simulation framework successfully fulfills its primary design objective: the real-time, physics-based determination of safe operating power envelopes for lithium-ion battery modules under dynamic cyclic conditions. The framework captures the nonlinear interdependencies between SOC, terminal voltage, internal resistance, and cell temperature within a unified, computationally tractable model, and translates these interdependencies into actionable, continuously updated power limit estimates. These properties collectively establish the proposed approach as a viable and practically deployable foundation for advanced power management in electric vehicle battery systems, stationary energy storage platforms, and any application domain where safe, efficient, and adaptive utilization of lithium-ion battery modules is required [2], [3], [4].

4. Conclusion

This study presented a simulation-based framework for the real-time estimation of dynamic charging and discharging power limits of a lithium-ion battery module under cyclic CC–CV operating conditions. The framework was developed within the MATLAB/Simulink environment using the Simscape Battery Toolbox R2025a and integrates three functionally coupled subsystems: an electro-thermal battery module model, a CC–CV charge–discharge controller, and a physics-based Battery Power Estimator block operating over a fixed 10-second prediction horizon.

The principal findings of the study can be summarized as follows.

Electro-thermal modeling fidelity. The developed 4S3P battery module model, incorporating SOC- and temperature-dependent open-circuit voltage and internal resistance parameters, successfully reproduced the salient electrochemical and thermal dynamics of lithium-ion cells under cyclic operation. The enabled thermal path captured the bidirectional coupling between heat generation, cell temperature, and internal resistance evolution — a coupling that proves indispensable for accurate power limit estimation under conditions deviating from nominal ambient temperature. The physical consistency of the model output across multiple successive charge–discharge cycles confirms that the simulation framework is free from numerical drift and initialization artifacts, and that it has attained a stable cyclic steady state representative of practical battery operation [2], [4].

SOC-dependent power capability. The simulation results demonstrated that both the maximum charging and maximum discharging power exhibit pronounced, nonlinear dependence on the state of charge. The allowable charging power is highest at low and intermediate SOC levels, where the voltage headroom between the terminal voltage and the upper threshold of 4.15 V is largest, and decreases sharply as the SOC approaches 90% due to intensifying electrochemical polarization and narrowing voltage margin. Conversely, the maximum discharge power peaks in the intermediate SOC range of approximately 50–70%, where the open-circuit voltage is elevated and the internal resistance is near its minimum, and diminishes rapidly at low SOC as voltage sag and increasing internal resistance constrain the permissible discharge current [2], [3]. These findings quantitatively characterize the asymmetric power capability envelope of the module and provide a physically grounded basis for SOC-aware power management in BMS control logic.

Performance of the Battery Power Estimator. The Battery Power Estimator exhibited stable, smooth, and physically consistent operation throughout the entire simulation interval. The 10-second prediction horizon proved to be a well-balanced design choice, providing sufficient responsiveness to rapid changes in current, voltage, and SOC while avoiding excessive sensitivity to short-duration transient fluctuations. The estimator enforced electrochemical safety boundaries proactively at both extremes of the SOC range — curtailing charging power near full charge to prevent overvoltage and lithium plating, and reducing discharge power near full depletion to prevent deep discharge and associated irreversible capacity loss — without requiring empirical calibration or offline parameter tuning [1], [3].

Advantages over conventional approaches. The physics-based estimation framework demonstrated clear advantages over conventional static lookup-table methods. By continuously integrating the instantaneous SOC, terminal voltage, internal resistance, and cell temperature within a unified predictive model, the proposed approach generates power limit estimates that adapt in real time to the evolving electrochemical and thermal state of the module. This adaptability is fundamentally unattainable by static methods, which cannot account for the coupled, time-varying nature of battery dynamics under realistic operating conditions [3], [4]. The proposed framework therefore addresses a well-documented limitation of current BMS practice and contributes a practically deployable solution to the field of advanced battery power management.

Practical applicability. The demonstrated properties of the framework — physical consistency, real-time adaptability, stable operation across the full SOC range, and reliable safety boundary enforcement — confirm its suitability for integration into intelligent BMS architectures

https://doi.org/10.56143/3030-3893-2026-2-83-92 A bridge between science and innovation

for electric vehicles, hybrid electric vehicles, and stationary energy storage systems. Direct application areas include adaptive charge control, regenerative braking power management, peak power limitation, thermal protection, and real-time safety monitoring. Furthermore, the physics-based power limit estimates generated by the framework constitute high-quality state information suitable for use as inputs to machine learning-based and model predictive control energy management algorithms, positioning the proposed approach as an enabling component for next-generation AI-assisted BMS platforms [2], [3], [4].

Limitations and future work. The present study is subject to several limitations that define directions for future investigation. First, the simulation was conducted under idealized cyclic CC–CV conditions with a fixed ambient temperature of 25°C; future work should evaluate estimator performance under variable temperature environments, stochastic drive cycle profiles, and multi-rate current inputs representative of real vehicular duty cycles. Second, the equivalent circuit model employed in this study, while computationally efficient, does not explicitly resolve the spatial distribution of lithium concentration within electrode particles; incorporation of a reduced-order electrochemical model — such as the single particle model (SPM) or its thermal extension — would improve the physical fidelity of the internal resistance and OCV representations, particularly at high C-rates [2]. Third, the effect of battery aging on estimator accuracy was not considered; as internal resistance increases and capacity decreases over the service lifetime of the module, the power limit estimates will require online parameter adaptation to remain valid. Future work should therefore investigate the integration of recursive parameter identification or data-driven aging correction mechanisms into the estimation framework. Finally, experimental validation of the simulation results against physical battery module test data would further strengthen the credibility and generalizability of the proposed approach.

References

[1] MathWorks. Battery Power Estimator — Simscape Battery Toolbox R2025a Documentation. MathWorks, Inc., 2025. [Online]. Available: https://www.mathworks.com/help/simscape-battery/

[2] Plett G. L. Battery Management Systems: Volume I – Battery Modeling. — Artech House, 2015. — 344 p.

[3] Hu X., Jiang J., Egardt B. Advanced Estimation Techniques for Lithium-Ion Battery Management // IEEE Transactions on Industrial Electronics. — 2015. — Vol. 62. — No. 8. — pp. 4173–4182.

[4] Pesaran A. A. Battery Thermal Models for Hybrid Vehicle Simulations // National Renewable Energy Laboratory (NREL). — 2002. — Tech. Rep. NREL/CP-540-30149.

[5] Waldmann T., Wilka M., Kasper M., Fleischhammer M., Wohlfahrt-Mehrens M. Temperature dependent ageing mechanisms in Lithium-ion batteries — A Post-Mortem Study // Journal of Power Sources. — 2014. — Vol. 262. — pp. 129–135.

[6] Doyle M., Fuller T. F., Newman J. Modeling of Galvanostatic Charge and Discharge of the Lithium/Polymer/Insertion Cell // Journal of The Electrochemical Society. — 1993. — Vol. 140. — No. 6. — pp. 1526–1533.

[7] Xiong R. Battery Management Algorithm for Electric Vehicles. — Springer, 2020. — 281 p.

[8] Liaw B. Y., Nagasubramanian G., Jungst R. G., Doughty D. H. Modeling of lithium ion cells — A simple equivalent-circuit model approach // Solid State Ionics. — 2004. — Vol. 175. — No. 1–4. — pp. 835–839.

[9] Lin X., Perez H. E., Mohan S., Siegel J. B., Stefanopoulou A. G., Ding Y., Castanier M. P. A lumped-parameter electro-thermal model for cylindrical batteries // Journal of Power Sources. — 2014. — Vol. 257. — pp. 1–11.

[10] Bernardi D., Pawlikowski E., Newman J. A general energy balance for battery systems // Journal of The Electrochemical Society. — 1985. — Vol. 132. — No. 1. — pp. 5–12.

Information about the author

Igor Kolesnikov	Toshkent davlat transport universiteti "Elektrotexnika" kafedrasi professori, t.f.d., (DSc) E-mail: kolesnikovigor1944@gmail.com Tel.:+998903737356 https://orcid.org/0009-0009-2998-3964
Karimberdi Karshiev	Toshkent davlat transport universiteti "Elektrotexnika" kafedrasi assistent. E-mail: karimberdiqarshiyev@gmail.com Tel.: +998993003696 https://orcid.org/0000-0001-5275-5200

https://doi.org/10.56143/3030-3893-2026-2-83-92

CONTEXT / MUNDARIJA